Transport studies of perovskite oxide $BaPb_{1-x}Zr_xO_3$

2000 J. Phys.: Condens. Matter 12 933

(http://iopscience.iop.org/0953-8984/12/6/315)

J. Phys.: Condens. Matter **12** (2000) 933–942. Printed in the UK PII: S0953-8984(00)03889-3

Transport studies of perovskite oxide $BaPb_{1-x}Zr_xO_3$

Y D Zhao†‡‖, Y T Qian†‡, H Zhang§, P F Yang§, K B Tang†‡, Y Z Ruan§ and Y H Zhang†

† Structure Research Laboratory, University of Science and Technology of China, Hefei 230026, People's Republic of China
‡ Department of Chemistry, University of Science and Technology of China, Hefei 230026, People's Republic of China
§ Department of Material Science and Engineering, University of Science and Technology of China, Hefei 230026, People's Republic of China

Received 4 June 1999, in final form 29 September 1999

Abstract. We have synthesized perovskite oxide $BaPb_{1-x}Zr_xO_3$ by solid-state reaction in different atmospheres and performed x-ray diffraction (XRD) analyses, electrical resistivity and thermoelectric power measurements on them. Nearly single-phase samples with cubic symmetry were obtained in the range $0.0 < x \leqslant 0.25$. As x increased, a metal–insulator (MI) transition occurred at a critical doping level x_c, which depended on the sintering atmosphere of the samples. Meanwhile, a jump in resistivity was found. At low temperatures (13 K $\leqslant T \leqslant$ 100 K), the temperature dependence of resistivity followed the power law when $0 < x < x_c$ and the hopping law when $x \geqslant x_c$. When prepared in oxygen and in air, the resistivity decreased linearly with the rising temperature in the range between 100 and 300 K. However, the unusual linear behaviour was absent when the doped oxides were sintered in N_2. An anomalous broad peak was also observed in the thermoelectric power of the air-sintered samples. The results are discussed in terms of the effects of disorder and electron–electron interactions, oxygen vacancies and the crystal-field splitting of the 4d levels of transition metal Zr.

1. Introduction

The effects of disorder and electron–electron interactions on the electronic transport properties of materials are important topics of considerable interest. A critical degree of disorder can drive a good metal (and even a superconductor) into an insulator by localizing the electrons through quantum interference. On the other hand, sufficiently strong interactions between electrons can split the half-filled band of a metal and open a gap. In a real system, the two kinds of effects often interplay. When the effects of disorder dominate, the metal to insulator (MI) transition is called the Anderson transition. When the electron–electron interactions dominate, the MI transition is labelled the Mott–Hubbard transition. On the metallic side of the MI transition, one usually sees the $T^{1/2}$ dependence of resistivity that arises from both disorder and interactions [1]. On the insulating side, one may observe variable range hopping (VRH) behaviour [2] or correlated hopping behaviour [3], which are respectively driven by intrasite Coulomb repulsion and long-range interaction between electrons in the presence of disorder. These anomalous transport phenomena were observed in the V_2O_3 system [4], sodium tungsten bronze [5] and perovskite oxides of transition metals [6].

‖ Corresponding author.

0953-8984/00/060933+10$30.00

Note that $BaPbO_3$ is a metallic perovskite oxide containing no transition-metal ions. Its resistivity has a small temperature-dependent part. After Bi was doped into the Pb sites, superconductivity occurred at about 13 K along with an MI transition which coincided with structural changes [7, 8], whereas, when Sb was introduced into the Pb sites, no MI transition was found [9]. The material remained metallic although its resistivity was enhanced by the doping of Sb. Considering the fact that transition-metal ions have various d electronic configurations, it would be interesting to find if the anomalous transport phenomena is also present in the $BaPbO_3$ system when transition-metal ions are doped into the Pb sites. In this work, we report experimental results of transport properties in perovskite oxides $BaPb_{1-x}Zr_xO_3$. We observed a jump in resistivity when x reached a certain value, x_c, as well as an unusual linear behaviour of resistivity with a negative temperature coefficient at high temperatures. We also observed the salient influence of a sintering atmosphere on the transport properties.

2. Experimental

The samples used were sintered ceramic pellets prepared by solid-state reaction. Reagents of $BaCO_3$ (99.9%), PbO_2 (99.9%) and ZrO_2 (99.9%) were used as starting materials. The stoichiometric mixtures of starting powders were thoroughly ground and heated in air at 800 °C for 12 h. The heating rate was about 4 °C min^{-1}. The calcined mixtures were reground and fired at 950 °C for 20 h and the obtained powders were pressed into disk-shaped pellets (of diameter 10 mm and thickness 2 mm) and refired in flowing O_2 or air at 980 °C for 20–24 h. This was followed by furnace cooling (at a rate of about 5 °C min^{-1}) to room temperature. Some samples were sintered in N_2 at 1000 °C for 24 h, then step-cooled to 800 °C, 50 °C per step (the cooling rate was about 30 °C min^{-1}, the staying time at each step was 2 h) and then furnace-cooled to room temperature. The identification of phases in samples and the determination of lattice parameters were carried out on a Rigaku Dmax x-ray diffractometer using high intensity Cu Kα radiation, 40 kV accelerating voltage and 100 mA working current. Highly pure KCl powder was used as an internal standard for the determination of lattice parameters. Dc resistivity measurements were made in the temperature range between 13 and 300 K by the standard four-probe technique using a current of 1 mA. The temperature was determined using a calibrated Rh/Fe resistance thermometer and the voltage was recorded by a Keithly 181 nanovoltmeter (Keithly Instruments, Inc.; the resolution being 10^{-9} V). Electrical contacts were made by pressing highly pure indium grains on the cleaned surface of the sample. Special care was taken to avoid non-ohmic contacts. The thermoelectric power was measured by a differential method. The two ends of the bar-shaped sample ($6 \times 2 \times 1$ mm^3) were fixed with gelatin on two separated copper blocks through which two heating circuits kept the ends of the sample at different temperatures. The temperature gradient (ΔT) across the sample was measured using two pairs of copper–constantan thermocouples and its magnitude was kept at 2 K throughout the measurement. The thermocouples were soldered onto the copper blocks. The emf of the sample was recorded by a Keithly 181 nanovoltmeter. To eliminate the effects from the reference lead (Cu wires), the absolute thermoelectric power of Cu was subtracted from the measured thermoelectric voltage.

3. Results and discussion

The XRD analyses showed that nearly single-phase samples were obtained in the range $0 \leqslant x \leqslant 0.25$. The impurity phases increased with the rising Zr content, but did not exceed

Table 1. Lattice constant a of $BaPb_{1-x}Zr_xO_3$ at different doping levels.

x	0.0	0.10	0.15	0.20	0.25
a (nm)	0.42645	0.42612	0.42609	0.42605	0.42603

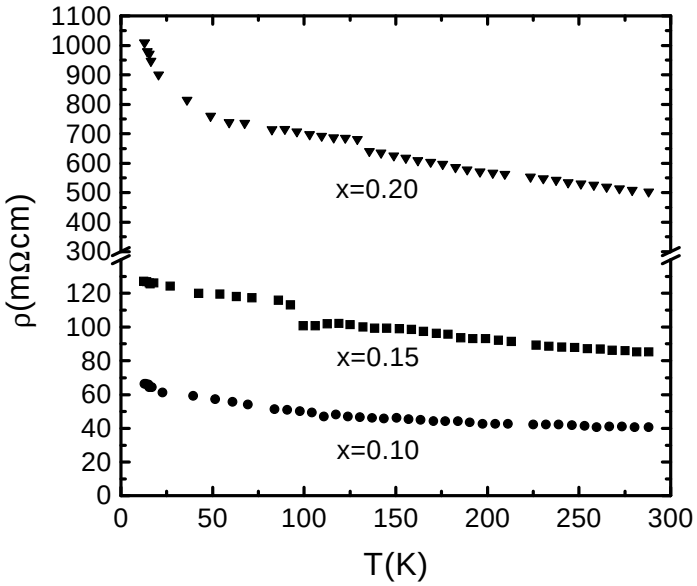

Figure 1. Temperature dependence of resistivity for the samples prepared in O_2.

5%. These samples showed cubic symmetry. No structural change was detected in the range $0 \leqslant x \leqslant 0.25$. In table 1 we list the composition dependence of lattice constant a. Obviously, the substitution of Pb^{4+} by smaller Zr^{4+} results in the reduction of the lattice constant with increasing x. Owing to the closeness in size, the introduction of Zr^{4+} does not bring about apparent distortion of the PbO_6 octahedra. In contrast, in $BaPb_{1-x}Bi_xO_3$, Bi disproportionates into Bi^{3+} and Bi^{5+}. The existence of larger Bi^{3+} gives rise to the distortion of the PbO_6 octahedra and therefore the structural changes.

Figure 1 shows the resistivity obtained for the $x = 0.1$, 0.15 and 0.20 samples which were sintered in O_2. It can be seen that the resistivity $\rho(T)$ increases with the rising Zr content x. When x reaches a certain value $x_c = 0.20$, a jump in resistivity is evident. When $x = 0$, $BaPbO_3$ has metallic type $\rho(T)$. As x increases, an MI transition takes place near x_c. The $x = 0.10$ and 0.15 samples are in the intermediate region. At high temperatures ($T > 100$ K), $\rho(T)$ depends linearly on temperature with a negative temperature coefficient. In figure 2 we show the linear fittings of resistivity at high temperatures. The fitting parameters are listed in table 2. At low temperatures (13 K $\leqslant T \leqslant$ 100 K), when $0 < x < x_c$, $\rho(T)$ obeys the power law $\rho(T) = \rho_1 + \beta T^n$, where β and n are two constants and ρ_1 is the extrapolated zero temperature resistivity. The best fits of the $x = 0.10$ and 0.15 data all give $n = 1/2$ (see figure 3). The fitting parameters ρ_1, β and the corresponding temperature ranges are also given in table 2. It can be seen that the $T^{1/2}$ behaviour persists over a wide temperature range. Using $\rho_1 \approx 3h\xi/4\pi e^2$, we estimate the coherence length $\xi \approx 120$ nm for $x = 0.10$ and $\xi \approx 220$ nm for $x = 0.15$. Such large coherence lengths indicate that the two samples are in the critical region of the MI transition. When $x \geqslant x_c$, we obtained a stretched exponential type

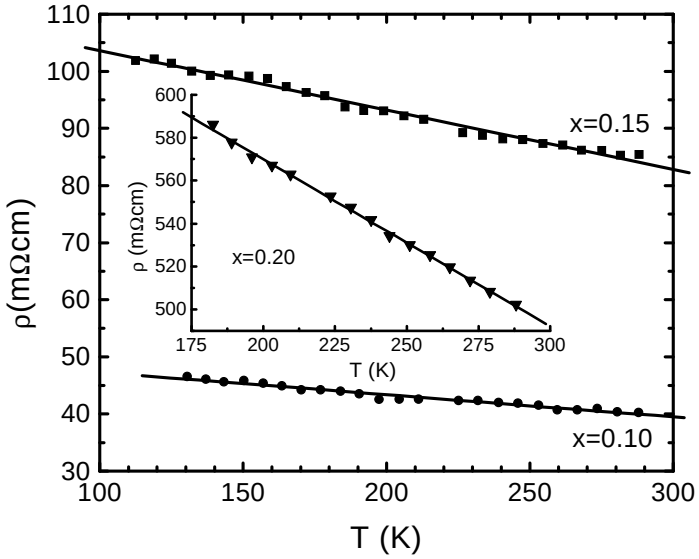

Figure 2. Linear fittings of resistivity according to $\rho = \rho_0 + \alpha T$ for the samples sintered in O_2 at high temperatures. The corresponding fitting parameters are listed in table 2.

Table 2. Linear fitting and $T^{1/2}$ law fitting parameters of resistivity for the samples sintered in O_2.

	$\rho = \rho_0 + \alpha T$			$\rho = \rho_1 + \beta T^{1/2}$		
x	ρ_0 (mΩ cm)	α (mΩ cm K^{-1})	T range (K)	ρ_1 (mΩ cm)	β (mΩ cm K$^{-1/2}$)	T range (K)
0.10	51.168	−0.0389	130.5–288	74.872	−2.5153	13–84
0.15	114.04	−0.1041	112.5–288	134.671	−2.1078	12.5–92.5
0.20	725.637	−0.7782	182.5–288			

of resistivity $\rho(T) = \rho_\infty \exp(T_0/T)^m$ for the $x = 0.20$ sample. The best fit gives $m = 1/2$ and $T_0 = 4.3$ K in the range 13 K $\leqslant T \leqslant$ 116 K (see the inset in figure 3). The exponent $m = 1/2$ indicates that $\rho(T)$ obeys the correlated hopping law [3]. This suggests that Coulomb interactions between electrons play a predominant role in the electronic transport of the above samples at low temperatures.

In figure 4, we show the resistivity for the samples which were sintered in air and furnace-cooled to room temperature. Compared with those samples sintered in oxygen, the resistivity almost remains unchanged for the $x = 0.1$ sample, but it is enhanced for the $x = 0.15$ sample. For the $x = 0.2$ sample, the resistivity is pronouncedly reduced along with the absence of the correlated hopping behaviour. When $x = 0.25$, the jump in resistivity takes place. At high temperatures, the linear behaviour of resistivity is retained in all samples (see figure 5). The fitting parameters are listed in table 3. At low temperatures, the best fits indicate that the $T^{1/2}$ law is followed for the $x = 0.1$, 0.15 and 0.2 samples (see figure 6) and the related fitting parameters are also given in table 3, while the stretched exponential law with $m = 1/4$ is held for the $x = 0.25$ sample (see the inset in figure 4).

Some samples were prepared by sintering in N_2 at 1000 °C for 24h followed by step-cooling to 800 °C, 50 °C per step, and then furnace-cooling to room temperature. Figure 7 shows the temperature dependence of resistivity for these samples. Compared with figure 4,

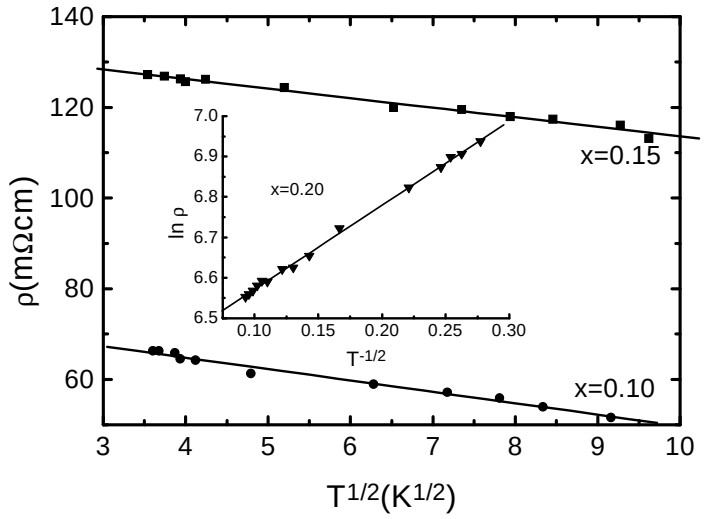

Figure 3. The $T^{1/2}$ behaviour for the $x = 0.10$ and 0.15 samples. The corresponding fitting parameters are listed in table 2. The inset shows the hopping behaviour $\rho(T) = \rho_\infty \exp(T_0/T)^{1/2}$ for the $x = 0.20$ samples.

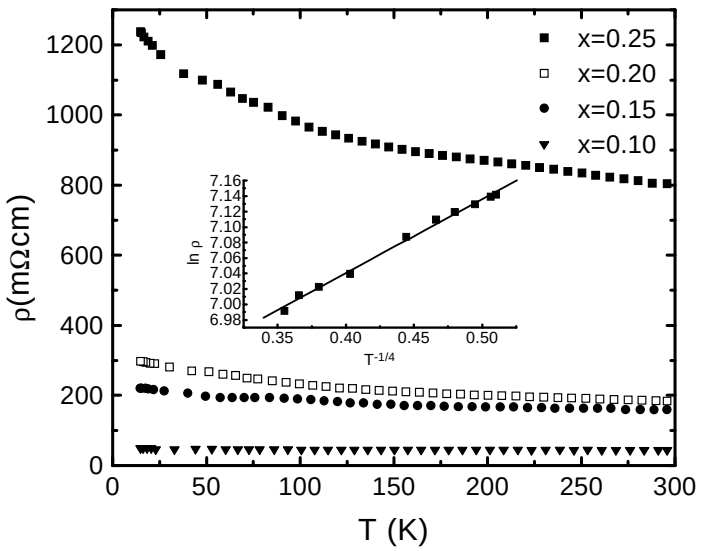

Figure 4. Temperature dependence of resistivity for the samples sintered in air. The inset shows the hopping behaviour $\rho(T) = \rho_\infty \exp(T_0/T)^{1/4}$ in the range 14.8 K $\leqslant T \leqslant$ 62.9 K for the $x = 0.25$ sample.

we can see that the jump in resistivity at $x = 0.25$ still exists. Preparation in N_2 does not change the magnitude of resistivity for the $x = 0.15$ and 0.2 samples. However, the resistivity of the $x = 0.25$ sample is enhanced by about tenfold, while that of the $x = 0.10$ sample is reduced by more than tenfold. Moreover, the temperature dependence of resistivity for this sample is changed to metallic type (see the inset in figure 7). Careful fits indicate that the $T^{1/2}$ law is still the best description of the resistivity behaviour at low temperatures for the

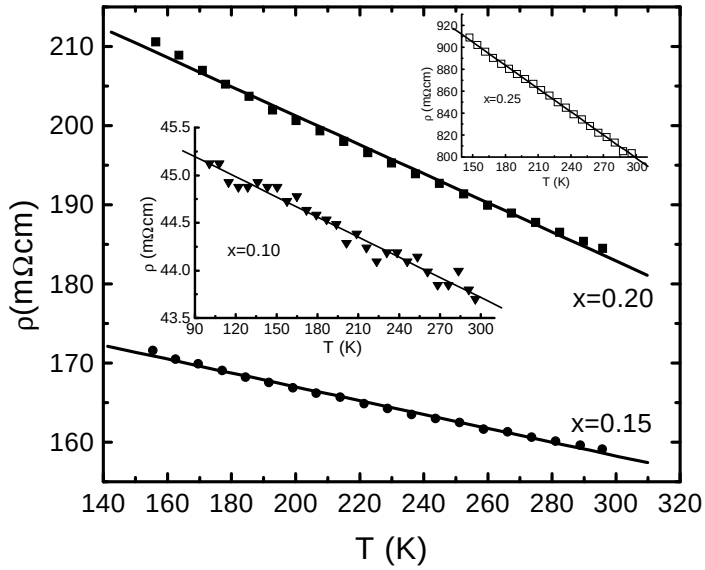

Figure 5. Linear fittings of resistivity according to $\rho(T) = \rho_0 + \alpha T$ for the samples sintered in air at high temperatures. The corresponding fitting parameters are listed in table 3.

Table 3. Linear fitting and $T^{1/2}$ law fitting parameters of resistivity for the samples sintered in air.

	$\rho = \rho_0 + \alpha T$			$\rho = \rho_1 + \beta T^{1/2}$		
x	ρ_0 (mΩ cm)	α (mΩ cm K^{-1})	T range (K)	ρ_1 (mΩ cm)	β (mΩ cm K$^{-1/2}$)	T range (K)
0.10	45.8295	−0.0071	100.7–295.8	52.9248	−0.9435	14.8–52.9
0.15	184.467	−0.0874	155.4–295.8	240.209	−5.237	14.8–105.8
0.20	238.032	−0.1838	156.4–295.8	339.891	−10.601	14.8–142.1
0.25	1010.815	−0.7066	147.2–295.8			

$x = 0.15$ and 0.2 samples (see figure 8). It is worth noting that the $T^{1/2}$ behaviour persists up to 224 K. The hopping law with $m = 0.1$ is obeyed by the $x = 0.25$ sample in the range from 15 K to 70 K (see the inset in figure 8). Strikingly, the linear temperature-dependent part of resistivity at high temperatures is absent in these samples. Evidently, sintering in N_2 pronouncedly changes the conduction behaviour of these samples.

It can be concluded that there are three features in these doped oxides. First, at low temperatures, the resistivity obeys the power law when $0 < x < x_c$ and the stretched exponential law with $0 < m < 1$ when $x \geqslant x_c$. These kinds of behaviour of resistivity are the manifestation of the effects of disorder and electron–electron interactions on electronic transport properties [10]. In these oxides, disorder mainly arises from the doping of Zr and the existence of oxygen vacancies. In the oxygen-sintered samples, as the doping level increases, disorder is enhanced. Thereby electrons diffuse more slowly and interact more strongly. In the intermediate regime ($0 < x < x_c$), the enhanced interaction causes the $T^{1/2}$ law at low temperatures [1, 11]. In the insulating regime ($x \geqslant x_c$), it leads to the opening of a small Coulomb gap in the state density near the Fermi level [3]. The existence of oxygen vacancies due to sintering in air and N_2 also gives rise to an additional disorder. The hopping behaviour changes from $m = 1/2$ in the O_2-sintered samples, $m = 1/4$ in the air-sintered

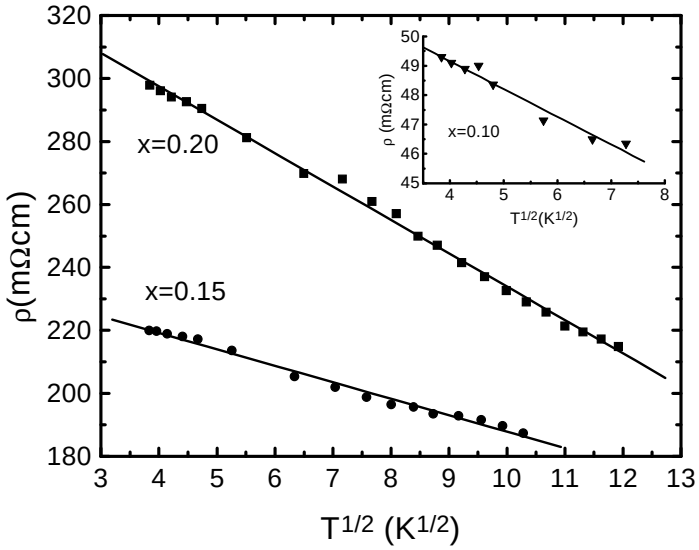

Figure 6. Power law fittings of resistivity according to $\rho(T) = \rho_1 + \beta T^{1/2}$ for the air-sintered samples at low temperatures. The corresponding fitting parameters are listed in table 3.

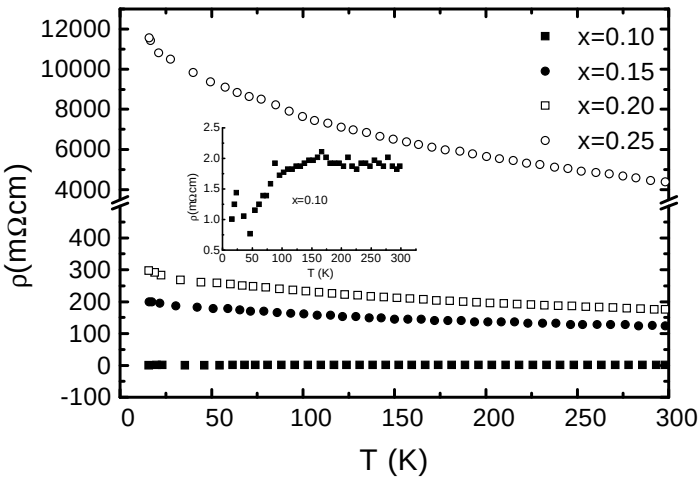

Figure 7. Temperature dependence of resistivity for the samples sintered in N_2. The inset shows that the conduction behaviour of the $x = 0.10$ sample changes to metallic type.

samples to $m = 0.1$ in the N_2-sintered samples, implying that the appearance of oxygen vacancies may modify the spectrum of available hopping states and/or the nature of the screening. Second, at high temperatures, an unusual linear behaviour of resistivity with a negative temperature coefficient is found on both the metallic side and the insulating side in all the samples except those sintered in N_2. Obviously, this kind of behaviour does not result from the same mechanism as the power law behaviour and the hopping behaviour at low temperatures because they are screened at high temperatures. The absence of this linear behaviour in N_2-sintered samples also implies that the formation of the linear behaviour is

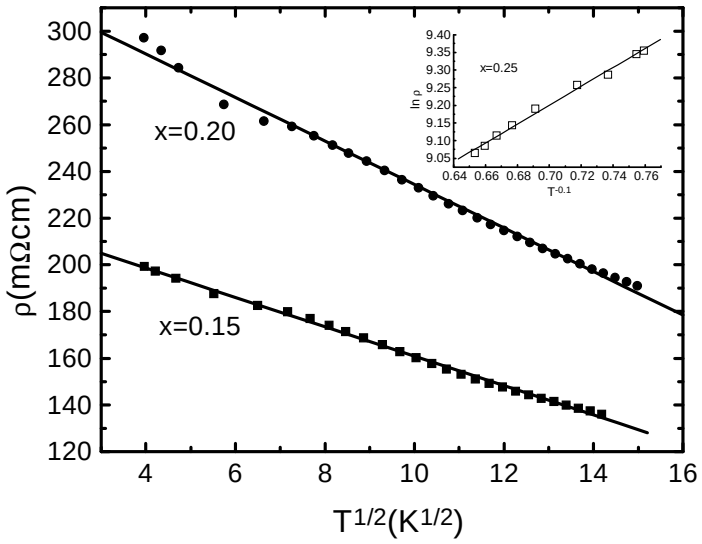

Figure 8. Power law fittings of resistivity according to $\rho(T) = \rho_1 + \beta T^{1/2}$ for the samples sintered in N_2. This behaviour persists over a wide temperature range. For $x = 0.15$, $\rho 1 = 223.873$ mΩ cm, $\beta = -6.297$ mΩ cm K$^{-1/2}$, $15.7K \leqslant T \leqslant 201.2$ K. For $x = 0.2$, $\rho_1 = 327.512$ mΩ cm, $\beta = -9.314$ mΩ cm K$^{-1/2}$, 15.7 K $\leqslant T \leqslant$ 224.6 K. The inset shows the hopping behaviour $\rho(T) = \rho_\infty \exp(T_0/T)^{0.1}$ in the range from 15.7 to 70.4 K for $x = 0.25$.

related to the amount of oxygen vacancies. Third, a jump in resistivity is also observed when the doping level reaches a certain value, x_c, which depends on the sintering atmosphere (20% for the oxygen-sintered samples and 25% for the air- or N_2-sintered samples).

Generally, anomalies in the behaviour of resistivity will be reflected in other transport properties such as thermoelectric power and magnetoresistance. We carried out thermoelectric power measurements on some samples. Figure 9 shows the temperature dependence of thermoelectric power (S) for the $x = 0.1$, 0.15 and 0.25 samples sintered in air. All samples have negative thermoelectric powers in the measured temperature range between 90 and 300 K, indicating that the charge carriers in these oxides are electrons. As the temperature goes down, S increases linearly for all samples, except for a broad peak which appears at around 270 K. All these S curves can be expressed as $S = A + B(1 - \lambda(T))T$, where A is the extrapolated zero temperature thermoelectric power and B the temperature coefficient. Their values are given in figure 9. $\lambda(T)$ is the temperature-dependent enhancement of S. When $T \leqslant 230$ K, $\lambda(T) = 0$ and when $T > 230$ K, $\lambda(T) > 0$. The linear temperature dependence of S is usually an indication of the metallic behaviour of samples with spherical Fermi surfaces [12]. This linear behaviour of S was also found in high-T_c superconducting oxides [13]. It seems that these samples behave like metals in the temperature range between 90 and 230 K. However, resistivity measurements showed that they are in the intermediate and the insulating regions. This suggests that these samples cannot be treated as simple metals. It should be mentioned that in spite of their big differences in resistivity, these samples behave similarly in S. The similarity implies that the linear behaviour of resistivity in these samples at high temperatures is an existing phenomenon. According to [14], corresponding to the VRH behaviour of resistivity, S is the sum of a linear term and a hopping term, i.e. $S = \alpha T + \beta T^{1/2}$. Unfortunately, we could not check this point in the $x = 0.25$ sample because our equipment could not reach further lower temperatures. The temperature-dependent enhancement $\lambda(T)$ is unexpected as

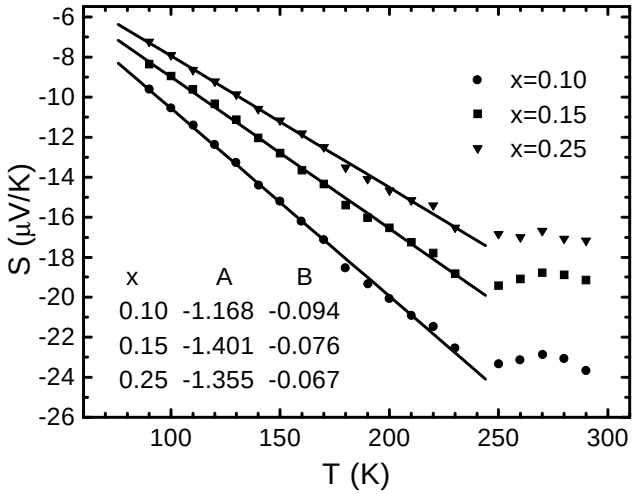

Figure 9. Temperature dependence of thermoelectric power S for the samples sintered in air. The solid lines show the linear behaviour $S(T) = A + BT$ in the range 90 K $\leqslant T \leqslant$ 230 K for the $x = 0.10$, 0.15 and 0.25 samples. The fitting parameters A and B are listed in this figure.

the anomaly is not observed in the corresponding resistivity measurements. It may be related to the existence of oxygen vacancies in these oxides. Further studies are needed to obtain a full understanding of the origin of the enhancement.

It is worth noting that the unusual linear behaviour and the jump in resistivity were not observed in $BaPb_{1-x}Sb_xO_3$ (while in $BaPb_{1-x}Bi_xO_3$, structural transitions made a notable contribution to the changes in conduction behaviour), where only s and p electrons are involved in the chemical doping. It is thereby reasonable to attribute these anomalies in transport properties to the introduction of the d electrons of transition-metal Zr. As pointed out in [15], the slight overlap of the empty Pb 6s band with the full O 2p band gives rise to the metallic conductivity of $BaPbO_3$. When Zr is doped into the Pb sites, it coordinates with six neighboring oxygen atoms forming an octahedron. The octahedral crystal-field splitting of the Zr 4d levels may bring about the closeness of the 4d sublevels and the Fermi level in energy, thereby leading to the hybridization of 4d sublevels and 2p (or 6s) band states. The hybridization will modify the width of the bands near the Fermi level and hence result in, if strong enough, a change in the conduction mechanism. When a sufficient amount of oxygen vacancies are present, the coordinating octahedron of Zr will be distorted, resulting in the modification of the crystal-field splitting and hence a change in the conduction behaviour. This may account for the disappearance of the linear behaviour and the recovery of the metallic behaviour when $x = 0.1$ in the N_2-sintered samples. Detailed band calculations based on this model may give more information.

In summary, we have carried out transport studies of the new perovskite oxide $BaPb_{1-x}Zr_xO_3$. A jump in resistivity accompanied by a composition-driven MI transition was found when x exceeds a certain value. The power law behaviour and the hopping behaviour of resistivity were observed at low temperatures. They are attributed to the effects of disorder and electron–electron interactions. An unusual linear behaviour with a negative temperature coefficient was also found at high temperatures when the samples were sintered in O_2 and air. However, this behaviour disappeared when the samples were prepared in N_2. These anomalies are related to the introduction of the d electrons of Zr. In addition, a broad peak at around

270 K was found in the thermoelectric power of the air-sintered samples. Its origin is unclear and warrants further studies.

References

[1] See, for example Rosenbaum T F and Carter S A 1982 *J. Solid State Chem.* **88** 94
Lee P A and Ramakrishnan T V 1982 *Phys. Rev.* B **26** 4009
Raychaudhuri A K 1995 *Adv. Phys.* **44** 21

[2] Mott N F 1969 *Phil. Mag.* **19** 639
Mott N F and Davis E A 1979 *Electronic Processes in Non-Crystalline Materials* 2nd edn (London: Oxford University Press)

[3] Efros A L and Shklovskii B I 1975 *J. Phys. C: Solid State Phys.* **8** L49
Efros A L 1976 *J. Phys. C: Solid State Phys.* C **9** 2021

[4] Rosenbaum T F and Carter S A 1990 *J. Solid State Chem.* **88** 94

[5] Raychaudhuri A K 1991 *Phys. Rev.* B **44** 8572

[6] Rajeev K P and Raychaudhuri A K 1992 *Phys. Rev.* B **46** 1309

[7] Sleight A W, Gillson J L and Biersteht P E 1975 *Solid State Commun.* **17** 27

[8] Thanh T D, Koma A and Tanaka S 1980 *Appl. Phys.* **22** 205

[9] Cava R J, Batlogg B, Espinosa G P, Ramirez A P, Krajewski J, Peck Jr W F, Rupp Jr L W and Cooper A S 1989 *Nature* **339** 291
Itch M, Sawada T, Kim I S, Inaguma Y and Nakamura T 1992 *Physica* C **204** 194

[10] Lee P A and Ramakrishnan T V 1985 *Rev. Mod. Phys.* **57** 287

[11] Chui T, Deutscher G, Lindenfeld P and McLean W L 1981 *Phys. Rev.* B **23** 6172

[12] Mott N F 1987 *Conduction in Non-Crystalline Materials* (London: Oxford)

[13] See, for example, Mandal J B, Das A N and Ghosh B 1996 *J. Phys.: Condens. Matter* **8** 3047

[14] Kaiser A B 1989 *Phys. Rev.* B **40** 2806

[15] Matheiss L F and Hamann D R 1982 *Phys. Rev.* **15** 4227